

Dominance effects and functional enrichments improve prediction of agronomic traits in hybrid maize

Guillaume P. Ramstein^{*}; Sara J. Larsson[†]; Jason P. Cook[‡]; Jode W. Edwards[§]; Elhan S. Ersoz^{**}; Sherry Flint-Garcia^{††}; Candice A. Gardner[§]; James B. Holland^{‡‡}; Aaron J. Lorenz^{§§}; Michael D. McMullen^{††}; Mark J. Millard[§]; Torbert R. Rocheford^{***}; Mitchell R. Tuinstra^{***}; Peter J. Bradbury^{†††}; Edward S. Buckler^{*,†††}; M. Cinta Romay^{*}

^{*} Institute for Genomic Diversity, Cornell University, Ithaca, NY, 14853

[†] Section of Plant Breeding and Genetics, Cornell University, Ithaca, NY, 14853. Current address: Corteva Agriscience, Windfall, IN, 46076

[‡] Division of Plant Science, University of Missouri, Columbia, MO, 56211. Current address: Department of Plant Sciences and Plant Pathology, Montana State University, MT, 59717

[§] USDA-ARS, Ames, IA, 50011. Department of Agronomy, Iowa State University, Ames, IA, 50011

^{**} Syngenta Seeds, Stanton, MN, 55018. Current address: Umbrella Genetics, Champaign, IL, 61820

^{††} USDA-ARS, Columbia, MO, 56211. University of Missouri, Columbia, MO, 56211

^{‡‡} USDA-ARS, Raleigh, NC, 27695. Dep. of Crop Science, North Carolina State University, Raleigh, NC, 27695

^{§§} Department of Agronomy and Horticulture, University of Nebraska, Lincoln, NE, 68588. Current address: Department of Agronomy and Plant Genetics, University of Minnesota, St Paul, MN, 55108

^{***} Department of Agronomy, Purdue University, West Lafayette, IN, 47907

^{†††} USDA-ARS, Ithaca, NY, 14853

Running title

Functional basis of genetic effects in hybrid maize

Keywords

Dominance, genomic features, functional enrichment, genomic prediction, hybrid maize

Corresponding authors

Guillaume P. Ramstein

175 Biotechnology Building

Ithaca, NY, 14853

+1 607 255 1809

gr226@cornell.edu

M. Cinta Romay

175 Biotechnology Building

Ithaca, NY, 14853

+1 607 255 1809

mcr72@cornell.edu

ABSTRACT

Single-cross hybrids have been critical to the improvement of maize (*Zea mays* L.), but the characterization of their genetic architectures remains challenging. Previous studies of hybrid maize have shown the contribution of within-locus complementation effects (dominance) and their differential importance across functional classes of loci. However, they have generally considered panels of limited genetic diversity and have shown little benefit from genomic prediction based on dominance or functional enrichments. This study investigates the relevance of dominance and functional classes of variants in genomic models, for agronomic traits in diverse populations of hybrid maize. We based our analyses on a diverse panel of inbred lines crossed with 2 testers representative of the major heterotic groups in the U.S. (1106 hybrids), as well as a collection of 24 biparental populations crossed with a single tester (1640 hybrids). We investigated three agronomic traits: days to silking (DTS), plant height (PH), and grain yield (GY). Our results point to the presence of dominance for all traits, but, also, among-locus complementation (epistasis) for DTS and genotype-by-environment interactions for GY. Consistently, dominance improved genomic prediction for PH only. In addition, we assessed enrichment of genetic effects in classes defined by genic regions (gene annotation), structural features (recombination rate and chromatin openness), and evolutionary features (minor allele frequency and evolutionary constraint). We found support for enrichment in genic regions and subsequent improvement of genomic prediction for all traits. Our results suggest dominance and gene annotations improve genomic prediction diverse populations in hybrid maize.

INTRODUCTION

Since the development of the first maize hybrids by Shull (1908) and their widespread adoption starting in the 1930s, hybrids have been central to the improvement of maize in the U.S.

Prevailing hypotheses about their advantage have focused on genomic complementation of parental genomes (Crow 1998). The basis for such complementation consists of non-additive genetic effects, particularly dominance (within-locus complementation, i.e., interaction between alleles within single genetic loci) and epistasis (among-locus complementation, i.e., interactions involving multiple genetic loci). Dominance was proposed as a major driver of genomic complementations in maize hybrids (Crow 1998, Lamkey and Edwards 1999). Epistasis also provides a plausible explanation for genomic complementation, but studies assessing its contribution to hybrid advantage have suffered from a lack of statistical power (Reif et al. 2005) and have reported conflicting results (e.g., Mihaljevic et al. 2005, Ma et al. 2007).

Genetic studies in maize have investigated dominance gene action by focusing either on directional dominance (consistent dominance effects across loci), effects of significant quantitative trait loci (QTL), or genome-wide polygenic effects. Studies on testcrosses or diallel mating designs seem to support the presence of directional dominance, particularly for grain yield (Reif et al. 2003, Hinze and Lamkey 2003). Furthermore, studies on populations derived from backcrosses between recombinant inbred lines and their parents have generally identified several QTL with significant dominance effects for traits such as flowering time, plant height, and grain yield (e.g., Frascaroli et al. 2007, Larièpe et al. 2012). However, genomic prediction analyses often did not show the contribution of dominance effects to genotypic variability, because they focused on populations of hybrids obtained from crosses between heterotic groups: Flint and Dent (e.g., Technow et al. 2014) or Stiff Stalk and non-Stiff Stalk (e.g., Kadam et al. 2016). Assessing the relevance of dominance effects in genomic prediction models would require more diverse panels in which complementation effects are more variable, due to differential degrees of complementarity within and across heterotic groups (Reif et al. 2005, Gerke et al. 2015).

The studies above have examined the relative importance of additive and dominance effects across the genome, but have not attempted to describe the properties of loci most enriched for causal variants: gene proximity, structural features, and/or evolutionary features. Gene proximity has been linked to causal variants in maize through enrichment for QTL effects in

genic regions (Wallace et al. 2014), consistent with a large portion of variability of gene expression being attributed to *cis* polymorphisms in maize (Schadt et al. 2003). Structural features such as chromatin openness and high recombination rate were also associated with enrichment for QTL effects in maize inbred lines (Rodgers-Melnick et al. 2016), but studies on hybrids have also shown that dominance effects could locate around centromeres, where recombination is low (Larièpe et al. 2012, Thiemann et al. 2014, Martinez et al. 2016). Evolutionary features reflecting low allelic diversity within species (allele frequency or nucleotide diversity) and across species (evolutionary constraint) have been associated with stronger QTL effects in hybrid maize (Mezmouk and Ross-Ibarra 2014, Yang et al. 2017). Importantly, structural and evolutionary features have also been associated with gene proximity (Beissinger et al. 2016, Rodgers-Melnick et al. 2016). Therefore, there is ambiguity about the relevance of evolutionary and structural features to capture variability at agronomic traits independently from gene proximity.

In this study, we characterized the genetic basis of three agronomic traits (days to silking, plant height, and grain yield) in panels representative of diversity in North-American hybrid maize. We analyzed two hybrid panels. One was derived from crosses between a diverse sample of maize inbred lines and either of two testers, B47 and PHZ51, belonging respectively to the Stiff Stalk (SS) and non-Stiff Stalk (NSS) heterotic groups. The other was derived from crosses between the US Nested Association Mapping (NAM) panel and PHZ51. Our study investigated the determinants of genotypic variability in hybrid maize, based on gene action (additive and/or dominance effects) or functional enrichments (by gene proximity and structural or evolutionary features) (Figure 1).

Hypothesis: Within-locus complementation			
Panel: Ames-H			
Prediction	DTS	PH	GY
Partition of variability by dominance effects	+	+	+
Dominance effects at QTL	N.S.	No QTL	No QTL
Linear effect of inbreeding	-	+	+
Gain in genomic prediction accuracy in NAM-H	N.S.	+	N.S.
Conclusion	DTS	PH	GY
Prevalent genetic dominance effects	-	+	+

Hypothesis: Functional importance of genic regions			
Panels: Ames-H, NAM-H			
Prediction	DTS	PH	GY
Partition of variability by gene proximity	+	+	+
Gain in genomic prediction accuracy across panels	+	+	+
Conclusion	DTS	PH	GY
Enrichment of genetic effects at gene-proximal loci	+	+	+

Figure 1 – Graphical summary of the study. We tested hypotheses regarding the statistical importance of two attributes about genomic variability in hybrid maize: (1) dominance effects; (2) functional enrichment of genetic effects in genic regions. Under each hypothesis, evidence from analyses is characterized as consistent (+) or inconsistent (-). Non-conclusive evidence is either due to absence of QTL (No QTL) or lack of significance (N.S.).

MATERIAL AND METHODS

Phenotypic data

Phenotypic measurements

In this study, two panels of maize lines were evaluated for hybrid performance: the NCRPIS association panel (hereafter, Ames) and the nested association mapping panel (hereafter, NAM). The Ames panel is a subset of temperate inbred lines from the diversity panel described by Romay et al. (2013); the NAM panel is a subset of 24 recombinant inbred line (RIL) populations, all having one parent in common, B73, as described by McMullen et al. (2009).

The hybrid Ames panel (Ames-H) was derived from a subset of 875 inbred lines which were selected to reduce differences in flowering time while favoring genetic diversity based on pedigree. Two inbred lines were selected as testers: one NSS inbred (PHZ51) and one SS inbred (B47, also known as PHB47). Inbreds were assigned to one or two testers based on known heterotic group: SS inbreds were crossed with PHZ51, while NSS inbreds were crossed with B47; inbreds with unknown heterotic group, as well as inbreds belonging to the Goodman association panel (Flint-Garcia et al. 2005) were crossed with both testers, for a total of 1,111 hybrids. The hybrid NAM panel (NAM-H) was developed as described by Larsson et al. (2017). Briefly, a subset of up to 80 RILs from each of the NAM families was selected to reduce differences in flowering time across families: the later RILs from the earliest families and the earlier RILs from the latest families, for a total of 1,799 RILs. All NAM RILs were crossed with the same tester, PHZ51.

In Ames-H, evaluations were performed in 2011 and 2012, in six locations across the US – Ames (IA), West Lafayette (IN), Kingston (NC), Lincoln (NE), Aurora (NY), and Columbia (MO) – for a total of nine environments: 11IA, 11IN, 11NC, 11NE, 11NY, 11MO, 12NE, 12NC, and 12MO. In NAM-H, hybrids were evaluated in five locations – Ames (IA), West Lafayette (IN), Kingston (NC), Aurora (NY), and Columbia (MO) – during 2010 and 2011 for a total of eight environments: 10IA, 10IN, 10NC, 10MO, 11IA, 11IN, 11NC, and 11NY. The following traits were measured in each hybrid panel: days to silking (number of days from planting until 50% of the plants had silks; DTS), plant height (cm from soil to flag leaf; PH), and grain yield (t/ha adjusted to 15.5% moisture; GY). In 11NY, only PH and DTS were measured (Table 1).

Both Ames-H and NAM-H panels were planted in two-row plots (40-80 plants per plot; 50,000 to 75,000 plants per hectare), except for 11NY, where 12 plants were planted per plot.

Phenotypic evaluations were conducted under augmented block designs, where blocking was used to reduce competition for light due to heterogeneous height and/or phenology (only checks were replicated within environments). In Ames-H, blocks were combinations of tester (PHZ51 or B47), maturity (early or late) and expected plant height (short, medium, or tall); checks were B73×PHZ51 (≤ 6 replicates per block) as well as PHZ51×B47, B47×PHZ51, and a maturity commercial check (each replicated once per block). In NAM-H, blocks were NAM families; checks were B73×PHZ51 (≤ 15 replicates per block) and the non-B73 parent crossed with PHZ51 (≤ 7 replicates per block) (Larsson et al. 2017).

Genotype means and heritability

For each combination of panel (Ames-H or NAM-H) and trait (DTS, PH, or GY), genotype means of hybrids were estimated by the following linear mixed model, fitted by ASREML-R v3.0 (Butler et al. 2009):

$$y_{ijkl} = g_i + (Env.)_{jk} + (Field)_{jkl} + s_{ijkl} + e_{ijkl}$$

where g_i was the mean of genotype i [fixed], $(Env.)_{jk}$ was the effect of location j and year k [random, independent, and identically normally distributed (i.i.d.)], $(Field)_{jkl}$ was the effect of field l within environment jk [random, i.i.d.], e_{ijkl} was the error [random, i.i.d.], and s_{ijkl} was a spatial effect within environment-field combinations [random, normally distributed under first-order autoregressive covariance structures by row and column]. Since genotypes were not replicated within environments, genotype-by-environment interactions were pooled with errors. For PH in both panels, spatial effects were not included in the model because the fitting algorithm could not converge to a solution. For GY in both panels, DTS measurements [fixed] were included in the model to account for phenological differences among lines. In addition to estimating genotype effects (g_i 's) as fixed, models with genotype effects as random were also fitted to estimate genotypic variance (σ_g^2) and error variance (σ_e^2). Broad-sense heritability on a plot basis was then calculated as $H^2 = \frac{\sigma_g^2}{\sigma_g^2 + \sigma_e^2}$. Finally, the average entry-mean reliability was

estimated as $r_g^2 = 1 - \frac{1}{n} \sum_{i=1}^n \frac{\text{Var}(g_i - \hat{g}_i)}{\sigma_g^2}$, where n is the number of hybrids evaluated in either

panel and $\text{Var}(g_i - \hat{g}_i)$ is the prediction error variance of the random genotype effect for hybrid i (Searle et al. 2009).

Genotypic data

Marker data

Marker scores (allele counts) at whole-genome-sequencing (WGS) SNPs in the Ames and NAM inbred panels were imputed from genotyping-by-sequencing (GBS) SNPs (Romay et al. 2013, Rodgers-Melnick et al. 2015), based on WGS SNPs in the Hapmap 3.2.1 reference panel (Bukowski et al. 2018), under version 4 of the B73 reference genome. Then, marker scores at WGS SNPs were inferred in Ames-H and NAM-H hybrids based on markers scores at their respective parents in the Ames and NAM inbred panels.

In the Ames and NAM inbred panels, GBS SNPs were called with the software TASSEL v5.0 (Bradbury et al. 2007) using the GBS production pipeline and the ZeaGBSv2.7 Production TOPM (Glaubitz et al. 2014). In the Hapmap 3.2.1 reference panel, WGS SNPs were processed as follows: 25,555,019 SNPs were selected (2 alleles per SNP, call rate $\geq 50\%$, and minor allele count ≥ 3), heterozygous marker scores were set to missing (since these were presumably due to errors or collapsed paralogous loci), and their missing marker scores were imputed. Marker scores at WGS SNPs in the Ames and NAM inbred panels were then imputed based on GBS SNPs (separately by panel), using the Hapmap 3.2.1 panel WGS SNPs as reference. Imputations of marker scores at WGS SNPs were performed by BEAGLE v5 (Browning and Browning 2018), with 10 burn-in iterations, 15 sampling iterations, and effective population size set to 1,000.

After imputation, $m = 12,659,487$ WGS SNPs were selected for estimated squared correlation between imputed and actual marker scores (≥ 0.8 ; Browning and Browning 2009) and minor allele frequency (≥ 0.01), in each combination of inbred panel and tester (e.g., set of Ames inbreds crossed to PHZ51), to avoid SNPs private to any of these sets. Marker scores at selected WGS SNPs were then inferred for each hybrid by CreateHybridGenotypesPlugin in TASSEL v5.0. The marker data at selected WGS SNPs in Ames-H ($n = 1106$) and NAM-H ($n = 1640$) consisted of the matrix \mathbf{X} of minor-allele counts, where minor alleles were defined by frequencies in the Hapmap 3.2.1 panel, and the matrix \mathbf{Z} of heterozygosity, which coded homozygotes as 0 and heterozygotes as 1.

Population principal components

Principal component analysis (PCA) was performed using the R package irlba v2.3.3 (Baglama and Reichel 2005) in the Goodman panel representing the genetic diversity among elite maize inbred lines (Flint-Garcia et al. 2005). The first three principal components (PCs) were computed based on allele counts at selected WGS SNPs (4.7%, 3.2% and 2.1% of genomic variability explained in the Goodman panel, respectively). The matrix \mathbf{P} of coordinates at the first three PCs in Ames-H and NAM-H was obtained by (i) adjusting allele counts by their observed mean in the Goodman panel, and (ii) mapping adjusted allele counts to PCs by SNP loadings, i.e., $\mathbf{P} = (\mathbf{X} - \mathbf{M})\mathbf{V}$, where $\mathbf{X} - \mathbf{M}$ is the matrix of adjusted allele counts in hybrid panels and \mathbf{V} is the $m \times 3$ matrix of right-singular vectors from the PCA.

Functional features

Gene annotation: proximity to genes

Gene positions were available from v4 gene annotations, release 40

([ftp://ftp.ensemblgenomes.org/pub/plants/release-](ftp://ftp.ensemblgenomes.org/pub/plants/release-40/gff3/zea_mays/Zea_mays.AGPv4.40.gff3.gz)

[40/gff3/zea_mays/Zea_mays.AGPv4.40.gff3.gz](ftp://ftp.ensemblgenomes.org/pub/plants/release-40/gff3/zea_mays/Zea_mays.AGPv4.40.gff3.gz)). Gene proximity bins (either ‘Proximal’ or ‘Distal’) indicated whether any given SNP was within 1 kb of an annotated gene (less than 1 kb away from start or end positions).

Structural features: recombination rate and chromatin openness

Published recombination maps identified genomic segments originating from either parent within the progeny of each NAM family (Rodgers-Melnick et al. 2015). These maps were uplifted to version 4 of the reference genome using CrossMap v0.2.5 (Zhao et al. 2014). Then, the recombination fractions were fitted on genomic positions by a thin-plate regression spline model, using the R package mgcv v1.8-27 (Wood 2003). Based on this model, recombination rates \mathbf{c} were inferred by finite differentiation of fitted recombination fractions: $\mathbf{c} = f\left(\mathbf{s} + \frac{1}{2}\right) - f\left(\mathbf{s} - \frac{1}{2}\right)$, where \mathbf{s} is the vector of genomic positions of all WGS SNPs, and f is the function inferred by the spline model. We defined recombination bins as follows: $c_j \leq 0.45$ cM/Mb, 0.45 cM/Mb $< c_j \leq 1.65$ cM/Mb, and 1.65 cM/Mb $< c_j$, where 0.45 cM/Mb and 1.65 cM/Mb are the first two tertiles of estimated recombination rates among all WGS SNPs.

Chromatin accessibility was measured by micrococcal nuclease hypersensitivity (MNase HS) in juvenile root and shoot tissues in B73 (Rodgers-Melnick et al. 2016). Here, MNase HS peaks were mapped to their coordinates in version 4 of the reference genome. A given SNP was considered to lie in a euchromatic (open) region if a MNase HS peak was detected, in either root or shoot tissues. We defined MNase HS bins as ‘Dense’ or ‘Open’ for the absence or presence of MNase HS peaks, respectively.

Evolutionary features: minor allele frequency and evolutionary constraint

Minor allele frequencies (MAF) at SNPs were determined based on the Hapmap 3.2.1 panel. Similarly to Evans et al. (2018), we defined MAF bins as follows: $MAF \leq 0.01$, $0.01 < MAF \leq 0.05$, and $0.05 < MAF$ (SNPs were not binned at $MAF \leq 0.0025$ due to only 7,202 of them falling into this class).

Evolutionary constraints at SNPs were reflected by genomic evolutionary rate profiling (GERP) scores (Davydov et al. 2010), derived from a whole-genome alignment of 13 plant species (Rodgers-Melnick et al. 2015, Yang et al. 2017), in version 4 of the reference genome. We defined GERP score bins by $GERP \leq 0$ and $GERP > 0$.

Genomic models

Polygenic additive effects (GBLUP)

Genome-wide additive effects were estimated under a genomic BLUP (GBLUP) model (VanRaden 2008), as follows:

$$\mathbf{g} = \mathbf{Q}\boldsymbol{\delta} + \mathbf{u} + \boldsymbol{\varepsilon}; \mathbf{u} \sim N(\mathbf{0}, \mathbf{G}\sigma_u^2), \boldsymbol{\varepsilon} \sim N(\mathbf{0}, \mathbf{I}\sigma_\varepsilon^2), \mathbf{G} = \mathbf{X}\mathbf{X}'/m$$

where \mathbf{g} was the vector of genotype means; $\mathbf{Q} = [\mathbf{1} \ \mathbf{P}]$ was the matrix consisting of a vector of ones and the three PCs as described above; $\boldsymbol{\delta}$ were fixed effects associated to \mathbf{Q} ; \mathbf{u} and $\boldsymbol{\varepsilon}$ consisted of polygenic additive effects and random errors, respectively; \mathbf{X} was the (non-centered) matrix of minor-allele counts at $m = 12,659,487$ WGS SNPs as described above. The GBLUP model was fitted in Ames-H or NAM-H, by restricted maximum likelihood (REML) using the R package regress v1.3-15 (Clifford and McCullagh 2005).

Polygenic additive and dominance effects (DGBLUP)

To account for dominance, the GBLUP model was extended to the dominance GBLUP (DGBLUP) model, as follows:

$$\mathbf{g} = \mathbf{Q}\boldsymbol{\delta} + \mathbf{u} + \mathbf{w} + \boldsymbol{\varepsilon}; \mathbf{u} \sim N(\mathbf{0}, \mathbf{G}\sigma_u^2), \mathbf{w} \sim N(\mathbf{0}, \mathbf{D}\sigma_w^2), \boldsymbol{\varepsilon} \sim N(\mathbf{0}, \mathbf{I}\sigma_\varepsilon^2), \mathbf{G} = \mathbf{X}\mathbf{X}'/m, \mathbf{D} = \mathbf{Z}\mathbf{Z}'/m \quad (1)$$

where \mathbf{w} consisted of polygenic dominance effects; \mathbf{Z} was the (non-centered) matrix of heterozygosity at $m = 12,659,487$ WGS SNPs as described above. Notably, in NAM-H, additive effects were completely confounded with dominance effects, because only one inbred tester was used in this panel (and only two genotype classes could exist at any given marker). Therefore, model (1) was fitted only in Ames-H, by REML using the R package regress v1.3-15 (Clifford and McCullagh 2005).

Directional effects

Under a simple dominance model without linkage or epistasis, inbreeding depression is characterized by a linear negative relationship between the inbreeding coefficient and fitness (Falconer and Mackay 1996). In the presence of directional epistatic effects, the relationship between the inbreeding coefficient and fitness is expected to be nonlinear (Crow and Kimura 1970). To capture such nonlinearity, especially dominance \times dominance epistasis, the quadratic effect of the inbreeding coefficient was fitted along with its linear effect, in genomic models. We followed Endelman and Jannink (2012) to estimate genomic inbreeding coefficients with respect to a base population, here represented by the Goodman panel. For each hybrid i , the coefficient of genomic inbreeding was calculated as $F_i = \frac{\sum_j (x_{ij} - 2\pi_j)^2}{\sum_j 2\pi_j(1-\pi_j)} - 1$, where π_j was the allele frequency in the Goodman panel.

Directional effects of inbreeding were analyzed as fixed effects under an extension of the DGBLUP model (1). The following model was fitted:

$$\mathbf{g} = \mathbf{Q}\boldsymbol{\delta} + \mathbf{R}\boldsymbol{\tau} + \mathbf{u} + \mathbf{w} + \boldsymbol{\varepsilon}; \mathbf{u} \sim N(\mathbf{0}, \mathbf{G}\sigma_u^2), \mathbf{w} \sim N(\mathbf{0}, \mathbf{D}\sigma_w^2), \boldsymbol{\varepsilon} \sim N(\mathbf{0}, \mathbf{I}\sigma_\varepsilon^2), \mathbf{G} = \mathbf{X}\mathbf{X}'/m, \mathbf{D} = \mathbf{Z}\mathbf{Z}'/m \quad (2)$$

where \mathbf{R} consisted of genomic inbreeding values (linear and quadratic); $\boldsymbol{\tau}$ were fixed effects associated to \mathbf{R} . Significance of $\boldsymbol{\tau}$ estimates was assessed by Wald tests. Model (2) was fitted in Ames-H, by REML using the R package regress v1.3-15 (Clifford and McCullagh 2005).

Oligogenic effects (GWAS)

To assess marginal additive effects (β_j , fixed, for each SNP j), the following model was fitted in Ames-H or NAM-H: $\mathbf{g} = \mathbf{Q}\boldsymbol{\delta} + \mathbf{x}_j\beta_j + \mathbf{u} + \boldsymbol{\varepsilon}$; $\mathbf{u} \sim N(\mathbf{0}, \mathbf{G}\sigma_u^2)$, $\boldsymbol{\varepsilon} \sim N(\mathbf{0}, \mathbf{I}\sigma_\varepsilon^2)$, $\mathbf{G} = \mathbf{X}\mathbf{X}'/m$.

Significance of SNPs was assessed by Wald tests on estimates of β_j . False discovery rates (FDR) were estimated based on p-values from Wald tests by the method of Benjamini and Hochberg (1995). In addition, posterior inclusion probabilities (PIP) were estimated by Bayesian sparse linear mixed models (BSLMM), fitted jointly on the whole matrix \mathbf{X} by GEMMA v0.98.1, with 1,000,000 and 10,000,000 MCMC iterations for burn-in and sampling, respectively (Zhou et al. 2013). Window posterior inclusion probabilities (WPIP) were subsequently estimated, following Guan and Stephens (2011), by summing PIPs in 500-kb windows, sliding by 250-kb steps. The most significant marker effects were then selected for $\text{FDR} \leq 0.05$ and $\text{WPIP} \geq 0.5$.

To assess additive and dominance effects (β_j and θ_j , fixed, for each SNP j), GWAS models were extended in Ames-H to incorporate dominance for both fixed effects and random effects: $\mathbf{g} = \mathbf{Q}\boldsymbol{\delta} + \mathbf{x}_j\beta_j + \mathbf{z}_j\theta_j + \mathbf{u} + \mathbf{w} + \boldsymbol{\varepsilon}$; $\mathbf{u} \sim N(\mathbf{0}, \mathbf{G}\sigma_u^2)$, $\mathbf{w} \sim N(\mathbf{0}, \mathbf{D}\sigma_w^2)$, $\boldsymbol{\varepsilon} \sim N(\mathbf{0}, \mathbf{I}\sigma_\varepsilon^2)$, $\mathbf{G} = \mathbf{X}\mathbf{X}'/m$, $\mathbf{D} = \mathbf{Z}\mathbf{Z}'/m$. Significance of SNPs was assessed by Wald tests on estimates of β_j and θ_j .

GWAS models were fitted under the EMMAX approximation of Kang et al. (2010), using function fastLm in the R package RcppEigen v0.3.3.5.0 (Bates and Eddelbuettel 2013).

Functional enrichments

Effects of functional features on the amplitude of marker effects were captured by linear mixed models which partitioned the genomic variance by annotation bins. For each feature (gene proximity, recombination rate, chromatin openness, MAF, and GERP) the following functional enrichment model was fitted:

$$\mathbf{g} = \mathbf{Q}\boldsymbol{\delta} + \mathbf{u} + \mathbf{w} + \boldsymbol{\varepsilon}; \mathbf{u} \sim N(\mathbf{0}, \sum_k \mathbf{G}_k \sigma_k^2), \mathbf{w} \sim N(\mathbf{0}, \sum_l \mathbf{D}_l \sigma_l^2), \boldsymbol{\varepsilon} \sim N(\mathbf{0}, \mathbf{I}\sigma_\varepsilon^2), \mathbf{G}_k = \frac{\mathbf{x}_k \mathbf{x}_k'}{m_k}, \text{ and}$$

$$\mathbf{D}_l = \frac{\mathbf{z}_l \mathbf{z}_l'}{m_l} \quad (3)$$

where \mathbf{X}_k (\mathbf{Z}_l) is the matrix of minor-allele counts (heterozygosity) at the m_k (m_l) SNPs in bin k (l), and σ_k^2 (σ_l^2) is the variance component associated to additive effects in bin k (dominance effects in bin l). The significance of variance partitions was assessed by likelihood ratio tests, comparing the REML of the evaluated model to that of a baseline model. Model (3) was fitted by REML using the R package regress v1.3-15 (Clifford and McCullagh 2005) in Ames-H or NAM-H. In NAM-H, model (3) did not include dominance effects (\mathbf{w}), because of collinearity of additive and dominance effects in this panel (due to only one inbred tester in NAM-H). Two types of variance partition were analyzed: partition by one feature (baseline: DGBLUP in Ames-H and GBLUP in NAM-H), and partition by both gene proximity and another feature (baseline: partition by gene proximity only in DGBLUP or GBLUP).

Variance partition and SNP enrichment

The proportion of variance explained by marker effects in GBLUP was estimated by

$$\frac{1}{n} \sum_i \frac{\tilde{G}_{ii} \sigma_u^2}{\tilde{G}_{ii} \sigma_u^2 + \sigma_\varepsilon^2},$$

where \tilde{G}_{ii} is the i^{th} diagonal element of matrix \mathbf{G} adjusted for fixed effects, i.e., $\tilde{\mathbf{G}} =$

$(\mathbf{I} - \mathbf{H})\mathbf{G}(\mathbf{I} - \mathbf{H})$, with $\mathbf{H} = \mathbf{Q}(\mathbf{Q}'\mathbf{Q})^{-1}\mathbf{Q}'$ being the matrix of projection onto the column space of \mathbf{Q} . The proportion of variance explained by additive marker effects in DGBLUP was

$$\text{estimated by } \frac{1}{n} \sum_i \frac{\tilde{G}_{ii} \sigma_u^2}{\tilde{G}_{ii} \sigma_u^2 + \tilde{D}_{ii} \sigma_w^2 + \sigma_\varepsilon^2},$$

and similarly for dominance effects, $\frac{1}{n} \sum_i \frac{\tilde{D}_{ii} \sigma_w^2}{\tilde{G}_{ii} \sigma_u^2 + \tilde{D}_{ii} \sigma_w^2 + \sigma_\varepsilon^2}$ [model

(1)], with $\tilde{\mathbf{D}} = (\mathbf{I} - \mathbf{H})\mathbf{D}(\mathbf{I} - \mathbf{H})$. In functional enrichment models, SNP enrichment for additive

effects at bin k^* was calculated by the ratio of $\left[\frac{1}{n} \sum_i \tilde{G}_{k^*ii} \sigma_{k^*}^2 \right] / \left[\frac{1}{n} \sum_i (\sum_k \tilde{G}_{kii} \sigma_k^2 + \sum_l \tilde{D}_{l ii} \sigma_l^2) \right]$,

i.e., the proportion of genomic variance explained by bin k^* , over $m_{k^*} / [\sum_k m_k + \sum_l m_l]$, i.e., the proportion of SNP effects in bin k^* (and similarly for dominance effects at bin l^*) [model (3)].

Validation of genomic prediction models

Prediction accuracy of genomic models (GBLUP, DGBLUP, GWAS models, and functional enrichment models) was characterized by the Pearson correlation between observed genotype means and their predicted values in validation sets. For models trained in Ames-H, a validation set was 1 of the 24 NAM-H populations. This validation scheme assessed prediction models for genomic selection in bi-parental breeding populations, and was compared to a “leave-one-population-out” cross-validation scheme where, for each validation set (population), models were trained on the remaining 23 populations in NAM-H. For models trained in NAM-H, a

validation set was 1 of 10 random subsets in Ames-H. These subsets were created by a random partition stratified by tester and population cluster (Figure S1), so that all validation sets equally represented variation over population clusters and testers. This validation scheme assessed prediction models for evaluation in diverse panels. The significance of prediction accuracy for any genomic model was tested for non-zero mean (by a one-sample t-test) and significant difference to another model (by a two-sample t-test paired by validation set).

Assessment of genotype-by-panel interactions

Interactions between genotypes and panels were assessed by Pearson correlation in genotype means between panels, for hybrids common to both panels (ρ_R). These hybrids were derived from crosses between PHZ51 and 1 of 23 reference lines (B73, B97, CML52, CML69, CML103, CML228, CML247, CML277, CML322, CML333, I114H, Ki3, Ki11, M162W, M37W, Mo17, Mo18W, NC350, NC358, Oh43, P39, Tx303, and Tzi8).

Genotype-by-panel interactions were also assessed by the following polygenic model, based on Jarquín et al. (2014):

$$\mathbf{g} = \tilde{\mathbf{Q}}\tilde{\boldsymbol{\delta}} + \tilde{\mathbf{u}} + \boldsymbol{\varepsilon}; \tilde{\mathbf{u}} \sim N(\mathbf{0}, \mathbf{G}\sigma_0^2 + [\mathbf{G} \circ \mathbf{E}\mathbf{E}']\sigma_1^2), \boldsymbol{\varepsilon} \sim N(\mathbf{0}, \mathbf{I}\sigma_\varepsilon^2), \mathbf{G} = \mathbf{X}\mathbf{X}'/m$$

where \mathbf{E} was the $n \times 2$ design matrix attributing genotypes to panels, either Ames-H or NAM-H; $\tilde{\mathbf{Q}} = [\mathbf{E} \ \mathbf{P}]$ and $\tilde{\boldsymbol{\delta}}$ captured effects of panels and population structure; $\tilde{\mathbf{u}}$ were polygenic genomic effects with main variance and panel-specific variance being quantified by σ_0^2 and σ_1^2 , respectively; \circ refers to the Hadamard (element-wise) product. For a given hybrid i , correlation in \tilde{u}_i between different panel j and j' was defined by $\rho_G = \text{Cor}(\tilde{u}_{ij}, \tilde{u}_{ij'}) = \frac{G_{ii}\sigma_0^2}{G_{ii}(\sigma_0^2 + \sigma_1^2)} = \frac{\sigma_0^2}{\sigma_0^2 + \sigma_1^2}$ (Jarquín et al. 2014). This model was fitted in Ames-H and NAM-H jointly, by REML using the R package regress v1.3-15 (Clifford and McCullagh 2005).

Data availability statement

Supporting data can be downloaded from <https://doi.org/10.25739/x2wc-yj71>: raw marker scores at GBS SNPs (Ames and NAM inbred panels), imputed markers scores at WGS SNPs (Hapmap3.2.1, Ames-H and NAM-H), raw phenotypic measurements (Ames-H and NAM-H), estimated genotype means (Ames-H and NAM-H), and functional annotations. Raw marker scores at WGS SNPs in Hapmap3.2.1 are publicly available (<https://doi.org/10.7946/p28h0c>;

Bukowski et al. 2018). Supporting code (in R and Bash) is available at https://bitbucket.org/bucklerlab/ames_nam_hybrid. Supporting information is available at figshare. Table S1 describes interactions between genotypes and environments. Table S2 describes high-confidence QTL effects in Ames-H and NAM-H, based on GWAS models and BSLMMs. Table S3 shows summary statistics about genomic inbreeding in Ames-H. Table S4 describes the difference in accuracy from Ames×PHZ51 to Ames×B47 for prediction in NAM-H. Table S5 describes prediction accuracy in NAM-H by directional effects of inbreeding in Ames-H. Table S6 describes prediction accuracy from GWAS models. Table S7 presents the significance of variance partition by panel and functional feature. Table S8 describes genomic heritability captured by functional classes in functional enrichment models. Table S9 describes genomic prediction accuracy of functional enrichment models. Figure S1 shows the population clusters in Ames-H, inferred by k-means clustering ($k = 4$). Figure S2 depicts linkage disequilibrium in Ames-H and NAM-H. Figure S3 shows allele frequency among female parents in Ames-H and NAM-H. Figure S4 shows the significance of marginal additive effects in GWAS in Ames-H and NAM-H. Figure S5 shows the SNP enrichment by bin, for structural and evolutionary features in Ames-H and NAM-H. Figure S6 shows the SNP enrichment by bin, for structural and evolutionary features in Ames-H and NAM-H, while accounting for enrichment by gene proximity.

RESULTS

Hybrid panels differ by genetic diversity and genetic basis for grain yield

Hybrid panels display contrasting levels of diversity

While the Ames hybrid panel (Ames-H) has a few hybrids with an affinity to semi-tropical lines like CML 247, it is, for the most part, comprised of hybrids closely related to SS lines like B73 and NSS lines like Mo17 (Figure 2). Compared to Ames-H, NAM-H is less diverse, since it was produced by crosses between a single NSS tester (PHZ51) and bi-parental populations which were all derived from a cross involving B73 as a common parent (NAM RILs are 50% B73). Moreover, female parents in NAM-H were selected for similar flowering time to PHZ51, hence further narrowing down the genetic diversity in this panel.

Genome-wide patterns of linkage disequilibrium and allele frequency are similar across panels

Linkage disequilibrium (LD) patterns are quite similar in both hybrid panels. After adjustment for population structure and relatedness (following Mangin et al. 2012), LD values are moderately concordant between Ames-H and NAM-H ($r = 0.77$) (Figure S2). Average LD values along chromosomes decay at similar rates, reaching 0.1 at 160 kb in Ames-H and 151 kb in NAM-H. Allele frequencies among female parents are also concordant between Ames-H and NAM-H ($r = 0.88$), but there are SNPs at low frequency in NAM-H (< 0.5) which segregate at frequencies between 0 and 1 in Ames-H (Figure S3).

Genetic architecture for grain yield differs across panels

Three agronomic traits were analyzed in Ames-H and NAM-H: days to silking (DTS), plant height (PH), and grain yield adjusted for differences in flowering time among hybrids (GY). The relatively low accuracy of genotype means for GY (as reflected by low broad-sense heritability and entry-mean reliability; Table 1) suggests variability due to genotype-by-environment interactions. Accordingly, genotypic effects for GY appear highly inconsistent across panels (Table S1). For GY, correlations across panels based on genotype means of reference lines (ρ_R) and genomic marker effects (ρ_G) are not significantly different from zero (p-value > 0.10 ; Table S1). In contrast, consistency in genetic bases is higher for PH ($\rho_R = 0.65$, $\rho_G = 0.78$; p-value < 0.001) and DTS ($\rho_R = 0.93$, $\rho_G = 1.0$; p-value < 0.001) (Table S1). Therefore, DTS, PH, and GY represent three distinct levels of sensitivity to genotype-by-environment interactions, being respectively weak, moderate, and strong.

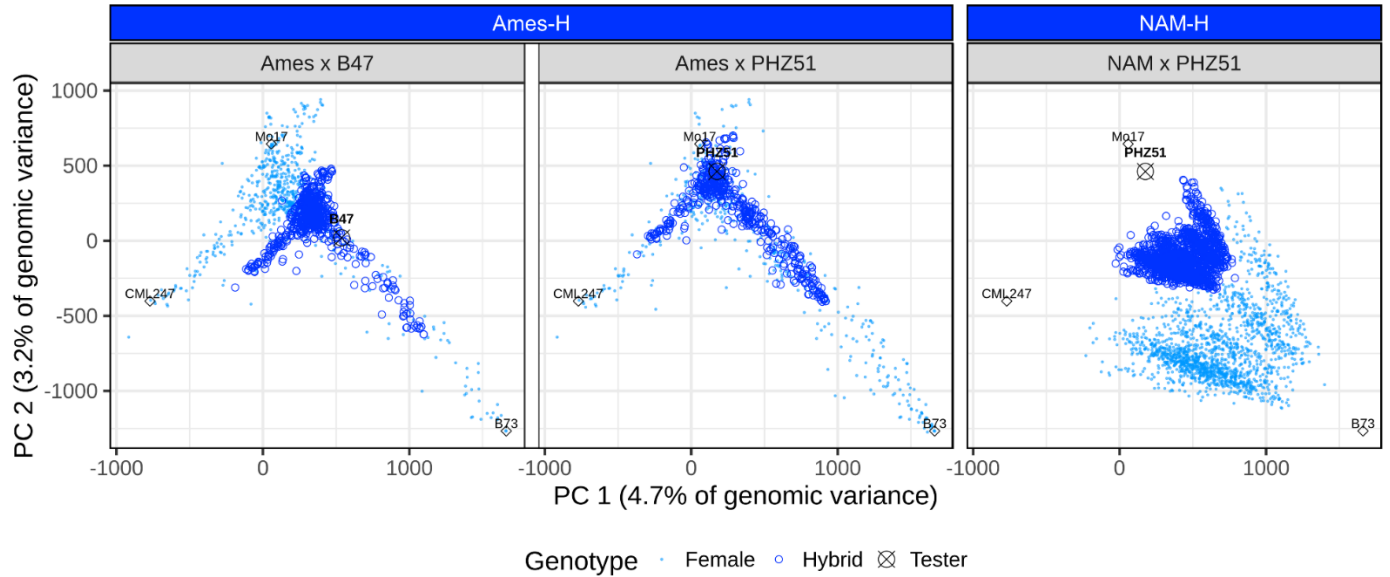


Figure 2 – The two hybrid panels differ by their number of testers and their level of diversity. *Principal component (PC) plot of hybrids. Ames-H consists of crosses between the Ames inbred panel and B47 (Ames×B47) or PHZ51 (Ames×PHZ51). NAM-H consists of crosses between the NAM inbred panel and PHZ51. Crossed circles refer to the male tester inbred line; light blue dots refer to female inbred lines; dark blue open circles refer to the hybrid lines making up Ames-H and NAM-H. Diamonds refer to reference lines: B73, SS reference line; Mo17, NSS reference line; CML247, CIMMYT semi-tropical reference line. Principal components and proportions of genomic variance explained were computed based on WGS SNPs in the Goodman panel.*

Table 1 – Phenotypic information by panel and trait

Panel	Trait	Environments	Mean	σ_g	H^2	r_g^2
Ames	DTS	11IA 11IN 11NC 11NE 11NY 11MO 12NC 12NE 12MO	66.4	2.1	0.78	0.95
		PH	219	13	0.69	0.92
		GY	6.13 [†]	0.66	0.29	0.62
NAM	DTS	10IA 10IN 10MO 11IA 11IN 11NC 11NY	70.6	1.5	0.55	0.81
		PH	247	10	0.30	0.69
		GY	6.94 [†]	0.44	0.16	0.35

Trait: days to silking (DTS), plant height (PH), grain yield adjusted for DTS (GY). Environments refer to year (2010, 2011, 2012) and locations [Kingston (NC), Ames (IA), West Lafayette (IN), Lincon (NE), Columbia (MO), and Aurora (NY)]. Mean: average phenotypic value; [†]: means shown for GY are adjusted by mean DTS. σ_g : genotypic standard deviation. H^2 : broad-sense heritability on a plot basis. r_g^2 : average entry-mean reliability.

Evidence for dominance effects in hybrids is consistent for plant height and grain yield

Analyses of dominance were conducted in Ames-H only. Under the hypothesis that dominance effects are pervasive in Ames-H, we expected consistent evidence for different types of dominance effects: polygenic effects from variance partition [*Material and methods*: model (1)]; fixed QTL effects from association mapping; directional effects from analysis of genomic inbreeding [*Material and methods*: model (2)]. Furthermore, we expected gains in genomic prediction accuracy to be achieved by any type of dominance effects in an extraneous panel (NAM-H) (Figure 1). Dominance effects of markers were not estimated in NAM-H because hybrids in this panel are characterized by only two genotype classes at any given marker (instead of three in Ames-H) such that additive and dominance effects are statistically equivalent in NAM-H.

Polygenic dominance effects capture genotypic variability for all traits

To assess the general relevance of polygenic dominance effects, genotypic variability was partitioned into additive and dominance components in a dominance GBLUP (DGBLUP) model. For all traits, dominance accounts for a significant portion of genotypic variability in Ames-H (p -value $\leq 2.2 \times 10^{-11}$), capturing 35%, 23%, and 41% of genomic variance for DTS, PH, and GY (Figure 3a). These estimates correspond to average degrees of dominance (ratio of dominance-to-additive standard deviations) of 0.73, 0.54, and 0.83 respectively. Therefore, overdominance does not seem to be pervasive in Ames-H (average degrees of dominance lower than one).

Effects of QTL are significant for days to silking but do not suggest dominance gene action

GWAS models reveal multiple significant QTL effects for DTS (Figure S4). There are five and seven high-confidence QTL ($FDR \leq 0.05$ and $WPIP \geq 0.5$; see *Material and methods*) for DTS in Ames-H and NAM-H, respectively (Figure S4; Table S2). For PH and GY, no QTL effects are significant except for one QTL in NAM-H for GY (Table S2). GWAS signals for DTS show limited consistency between Ames-H and NAM-H, with no overlap of high-confidence QTL across panels (Figure S4; Table S2).

To test whether dominance contributes to QTL effects, we conducted a GWAS for additive and dominance QTL effects in Ames-H. Multiple additive effects appear significant for DTS, with significant QTL effects ($FDR \leq 0.05$) in chromosomes 3, 1, and 9 (Figure 3c). But, dominance effects are not significant ($FDR > 0.30$) (Figure 3c), so the inconsistency in QTL effects for DTS across panels probably does not involve dominance. Moreover, genetic effects for DTS do not appear to be sensitive to environments (Table S1), and there are no systematic differences in allele frequency that consistently explain differences in significance of QTL effects across panels (Table S2). Thus, it is plausible that higher-order genetic interactions (epistasis) cause the difference in QTL significance for DTS across panels.

Effects of inbreeding point to higher-order genetic interactions for days to silking

Under directional dominance, inbreeding should be linearly related to fitness, but such relationship will tend to be nonlinear under higher-order epistatic interactions such as dominance \times dominance interactions (Crow and Kimura 1970). To test whether dominance contributes to genotypic variability by directional effects, we assessed linear and quadratic effects of genomic inbreeding (F) on agronomic traits. For PH and GY in Ames-H, only linear effects of genomic inbreeding are significant (Figure 3b; Table S3). Moreover, these effects are

on par with their expected impact on fitness, since genomic inbreeding is negatively associated with PH and GY. For DTS in Ames-H, only the quadratic effect of genomic inbreeding is significant (Figure 3b). Along with the lack of dominance QTL effects, this lack of linear effects suggests that non-additive genetic effects for DTS may not be properly captured by dominance effects, contrary to PH and GY where evidence from polygenic and directional effects is consistent.

Polygenic dominance effects increase prediction accuracy for plant height

Prediction accuracy within NAM-H (in leave-one-population-out cross-validation) is consistently higher than prediction accuracy from Ames-H to NAM-H, especially for GY (Table 2). Indeed, the observed decreases in prediction accuracy (between GBLUP trained in Ames-H and GBLUP trained in NAM-H) are larger when genomic correlations across panels are lower (Table S1). For DTS and PH, GBLUP models based on Ames-H (1106 hybrid crosses with PHZ51 or B47) are significantly more accurate than those based on Ames×B47 (subset of 643 hybrid crosses with B47 only), highlighting the benefit of having similar testers (PHZ51) between training and validation panels. Furthermore, GBLUP models based on Ames-H are as or more accurate than those based on Ames×PHZ51 (subset of 463 hybrid crosses with PHZ51 only), which demonstrates the robustness of GBLUP models to multiple testers within training sets. For GY, GBLUP models based on Ames×B47 are more accurate than those based on Ames-H or Ames×PHZ51 (Table 2). The close genetic relationship between B47 and the common parent in NAM-H, B73, may benefit prediction accuracy from Ames×B47 to NAM-H, despite the difference in tester (Figure 2). Moreover, the gain in prediction accuracy from Ames×PHZ51 to Ames×B47 is only significant in NAM-H populations which originate from tropical lines, at equal sample sizes (+0.124; p-value = 0.010; Table S4); therefore, female parents in Ames×B47 may also contribute to better predictions for GY, especially in NAM-H populations of tropical origin.

Incorporating dominance effects in GBLUP models results in significant gains in prediction accuracy for PH only (+0.023; p-value = 0.021), and no significant differences for DTS and GY (Table 2). Therefore, accounting for polygenic dominance effects should not be detrimental to genomic prediction models and may even increase their accuracy. In contrast, fixed effects do not contribute to increased prediction accuracy: directional effects from genomic inbreeding result in small and non-significant differences in prediction accuracy (Table S5);

additive and dominance effects at high-confidence QTL in GWAS models result in large and moderately significant decreases in prediction accuracy for DTS (-0.059; p-value < 0.10; Table S6).

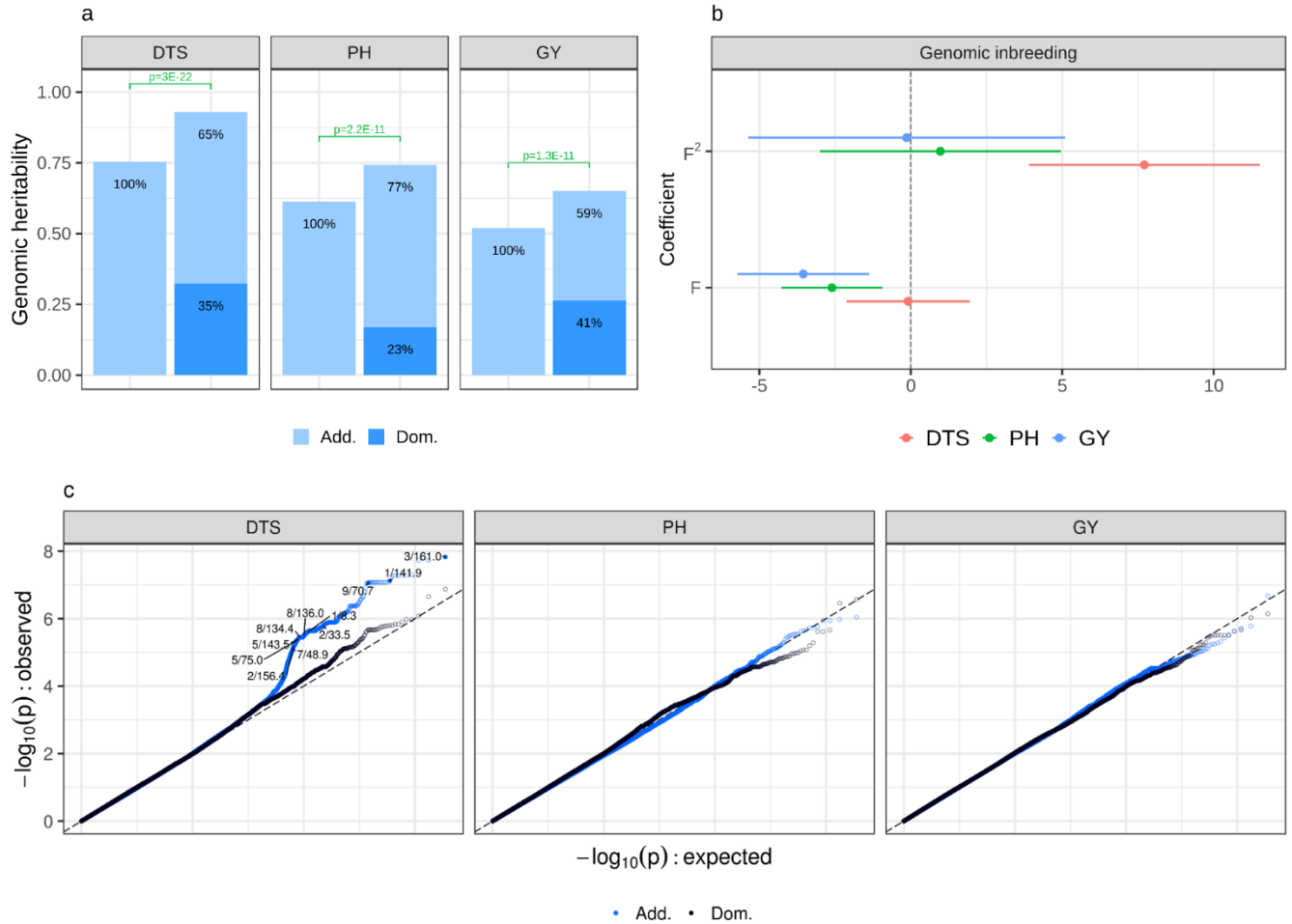


Figure 3 – Dominance genetic effects are prevalent for plant height (PH) and grain yield (GY), but not for days to silking (DTS), in Ames-H. (a) Partition of variance by additive and dominance effects in genome-wide polygenic models; genomic heritability: proportion of variance among genotype means captured by additive (Add.) or dominance (Dom.) marker effects; p: p-values from likelihood ratio tests. (b) Estimated effects of genomic inbreeding (point and 95% confidence interval). Effects are shown in unit of standard deviations for each trait. F: linear effect; F²: quadratic effect. (c) Quantile-quantile plot for joint estimates of additive effects ('Add.') and dominance effects ('Dom.'). Effects of SNPs were deemed significant if their false discovery rate (FDR) was lower than 0.05 and if they were not within 1 Mb of SNPs with more

significant effects (effects with lower p -values). SNPs with significant effects are designated by chromosome number and genomic position in Mb.

Table 2 – Genomic prediction accuracy in NAM-H

	Cross-validation prediction accuracy (p-value)	Prediction accuracy (p-value)	Difference in prediction accuracy (p-value)		
Training panel (testers)	NAM-H (PHZ51)	Ames-H (PHZ51, B47)	Ames-H (PHZ51, B47)	<u>Ames×PHZ51 (PHZ51 only)</u>	<u>Ames×B47 (B47 only)</u>
Model	GBLUP	GBLUP	<u>Dominance GBLUP</u>	GBLUP	GBLUP
DTS	0.405 (2.2×10^{-11})	0.331 (2.3×10^{-11})	-0.013 (0.21)	-0.028 (0.078)	-0.068 (2.7×10^{-3})
PH	0.394 (1.4×10^{-10})	0.235 (9.6×10^{-8})	+0.023 (0.021)	+0.014 (0.42)	-0.095 (8.5×10^{-5})
GY	0.240 (2.2×10^{-9})	-0.001 (0.96)	-0.010 (0.33)	-0.018 (0.29)	+0.056 (0.014)

Prediction accuracy: average correlation between observed and predicted phenotypes in NAM-H over 24 populations; Cross-validation prediction accuracy: leave-one-population-out prediction accuracy within NAM-H; Difference in cross-panel prediction accuracy: difference between models (dominance GBLUP vs. GBLUP model in Ames-H) or between training sets (Ames×PHZ51 or Ames×B47 vs. Ames-H). Significance of average prediction accuracies (non-zero mean) and estimated differences in prediction accuracy (non-zero difference, paired by NAM-H population) was assessed by t -tests.

Heterogeneity in polygenic effects is best captured by gene proximity

Analyses of functional features (gene proximity, recombination rate, chromatin openness, MAF and GERP scores) were conducted in Ames-H and NAM-H. Under the hypothesis that there are differential effects across functional classes, we expected SNP enrichment (enrichment in genomic heritability by class of SNPs) in functional enrichment models (partition of additive and dominance variance in Ames-H and partition of additive variance in NAM-H) [*Material and methods*: model (3)]. Moreover, we expected gains in prediction accuracy achieved by functional enrichment models across panels (Figure 1).

Polygenic effects are enriched in genic regions for all traits

Partition of genomic variance by proximity to annotated genes is significant for all traits in Ames-H and NAM-H, based on likelihood ratio tests combined by Fisher's method (p-value < 0.01; Table S7; Figure 4a). As suggested by the high correlation in significance ($-\log_{10}(\text{p-value})$) between Ames-H and NAM-H ($r = 0.92$), the higher significance of partitions in NAM-H could be due to a systematic increase in statistical power, due in part to the larger sample size in NAM-H ($n = 1640$ vs. $n = 1106$).

Polygenic SNP effects are consistently enriched near genic regions (Figure 4b), and the proportion of variance explained by gene-proximal SNPs is consistently larger than explained by gene-distal SNPs (56% to 100% of the genomic variability is explained by gene-proximal SNPs, across traits and panels; Table S8). Therefore, genetic effects seem enriched in genic regions, especially for PH where enrichment is highly significant in both panels.

Enrichment of polygenic effects by structural and evolutionary features is unclear

Partition of genomic variance explained by recombination rate, chromatin openness, MAF, and GERP scores is significant for DTS in NAM-H only, for PH in both panels (except MAF), and for GY in NAM-H only (except MAF) (Figure 4a; Table S7). SNP enrichments in both panels indicate that the magnitude of polygenic effects tend to be larger at low-diversity loci (low MAF and high GERP scores) and in euchromatic regions (open chromatin and moderate-to-high recombination rates) (Figure S5). However, none are significant across traits after accounting for gene proximity, based on likelihood ratio tests combined by Fisher's method (p-value > 0.01; Table S7). Because evolutionary constraint and chromatin structure are positively associated with gene density, enrichment at these features may be due to functional enrichment by gene proximity (Figure S6). One notable exception was MAF for GY (p-value = 9.8×10^{-3} ; Table S7), which indicates some promise for SNP enrichment by MAF classes. However, enrichments by MAF classes are inconsistent across panels, with rare SNPs ($\text{MAF} \leq 0.01$) being functionally enriched only in NAM-H, for example (Figure S6).

Variance partition by gene proximity or GERP scores increases prediction accuracy for all traits

Partitioning genomic variance by gene proximity is often useful to genomic prediction. From Ames-H to NAM-H (training in Ames-H, validation in NAM-H), partition of genomic variance by gene proximity increases prediction accuracy for DTS (+0.013, p-value = 3.3×10^{-4}), PH

(+0.029, p-value = 0.023), and GY (+0.010, p-value = 0.085), compared to a dominance GBLUP model (Figure 5). From NAM-H to Ames-H, partition by gene proximity increases prediction accuracy for PH only (+0.078, p-value = 1.1×10^{-4}), compared to a GBLUP model (Figure 5). Other features than gene proximity result in further gains in prediction accuracy (Table S9). In particular, partitioning genomic variance by GERP scores is useful for genomic prediction, even when accounting for enrichment by gene proximity, with significant gains in prediction accuracy achieved from NAM-H to Ames-H for DTS (+0.019, p-value = 1.6×10^{-4}) and GY (+0.040, p-value = 5.4×10^{-6}) (Figure 5). There are also some improvements by taking into account recombination rate (+0.014 for GY from Ames-H to NAM-H, +0.013 for DTS and +0.020 for GY from NAM-H to Ames-H), but they are less substantial than those achieved by using GERP scores (Table S9). Even when classes based on MNase HS and GERP scores do not yield significant gains in prediction accuracy, the high SNP enrichments achieved by taking into account these features (~32-fold for open-chromatin regions and ~8-fold for GERP > 0) can be of practical interest for SNP prioritization in genomic prediction (Figure S5; Table S8).

Improvements of prediction accuracy by enrichment of SNP effects in functional classes contrast with the lack of improvement from enrichment of SNP effects by GWAS. Incorporating high-confidence QTL effects from GWAS as fixed effects in either a dominance GBLUP model (from Ames-H to NAM-H) or a GBLUP model (from NAM-H to Ames-H) does not improve prediction accuracy, regardless of traits or validation schemes (Table S6; Figure 5). These results suggest that prioritizing few statistically significant loci (based on GWAS) may not be as useful as prioritizing broader classes of loci, probably because of background-dependency of strong QTL effects (marker-by-population and marker-by-environment interactions).

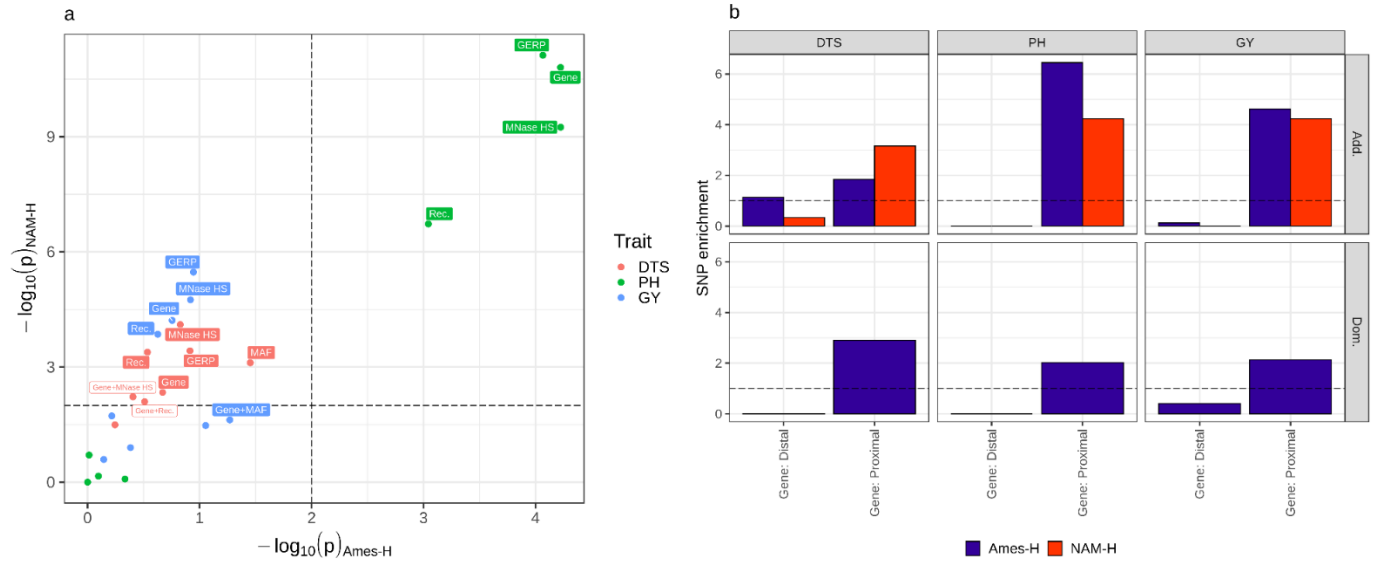


Figure 4 – Effects of SNPs are enriched in gene-proximal regions for days to silking (DTS), plant height (PH) and grain yield (GY), in Ames-H and NAM-H. (a) Significance of variance partition by gene proximity (Gene), structural features (Rec., MNase HS) or evolutionary features (MAF, GERP), and variance partition after accounting for gene proximity (Gene+Rec., Gene+MNase HS, Gene+MAF, Gene+GERP); p-values were obtained by likelihood ratio test comparing the functional enrichment model to a baseline model with no partition for the feature of interest (e.g. Gene vs. unpartitioned model, Gene+MAF vs. Gene); dashed lines correspond to thresholds for significance in either panel, after adjustment by Bonferroni correction. Labels refer to significant features after Bonferroni correction, based on p-values in either panel (open boxes) or p-values in both panels combined by Fisher’s method (full boxes) (Table S7). (b) SNP enrichment (inflation of SNP effects by functional class, i.e., the ratio of the proportion of genomic variance explained over the proportion of SNPs), for additive effects (Add.) and dominance effects (Dom.), by bin for gene proximity (Gene). Proximal: ≤ 1 kb of an annotated gene; Distal: > 1 kb from an annotated gene.

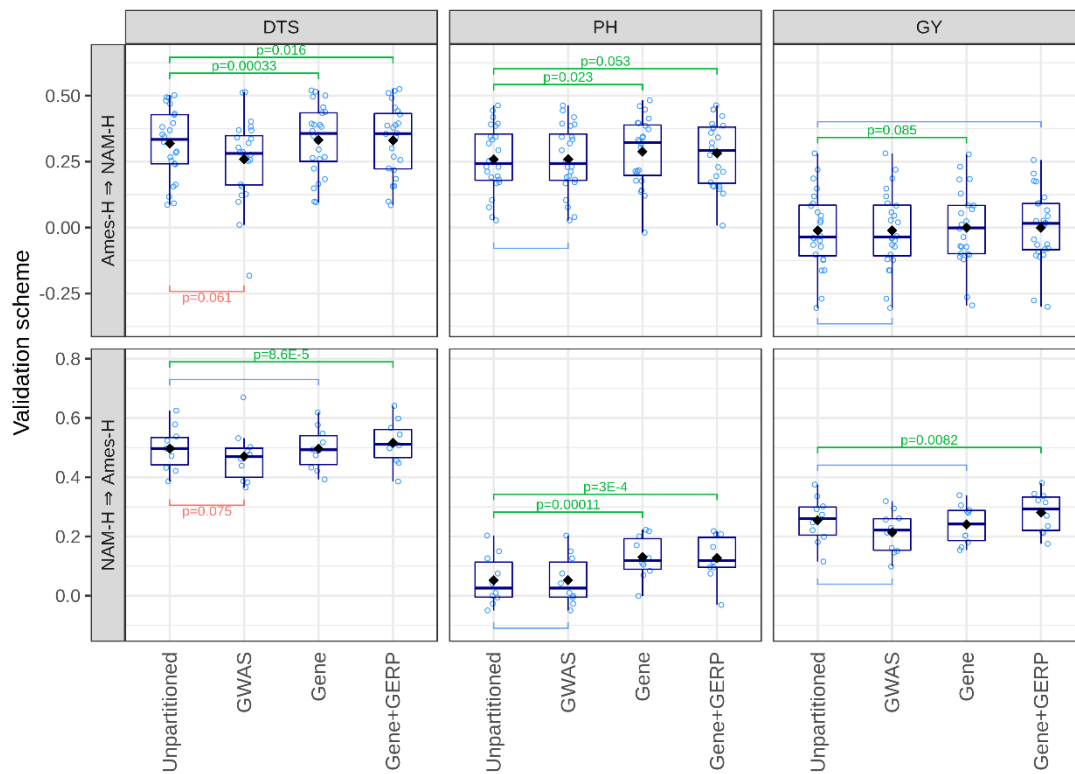


Figure 5 – Functional enrichment by gene proximity and GERP scores improve accuracy of genomic prediction models for days to silking (DTS), plant height (PH) and grain yield (GY).

Prediction accuracy (y-axis): average correlation between observed and predicted phenotypes in validation sets. Validation scheme: training panel \Rightarrow validation panel.

Unpartitioned: DGBLUP (polygenic additive and dominance effects) in Ames-H, GBLUP (polygenic additive effects only) in NAM-H; GWAS, fixed effects at high-confidence QTL from GWAS; Gene, functional enrichment by proximity to genes (≤ 1 kb of an annotated gene); Gene+GERP, functional enrichments by proximity to genes and GERP scores. Black diamonds indicate average prediction accuracy. Significance of estimated differences in prediction accuracy (non-zero difference) was assessed by t-tests, paired by validation set. Only p-values lower than 0.10 are shown.

DISCUSSION

Do additive and dominance effects adequately capture genetic architectures?

For all traits, a significant proportion of variance is explained by dominance effects (Figure 3a). However, for DTS, there is conflicting evidence about the importance of dominance: (i) no significant dominance QTL effects despite significant additive QTL effects (Figure 3c) and (ii) significant quadratic effects of genomic inbreeding, without any linear effect (Figure 3b). Such evidence indicates that DTS should probably be analyzed under more complex genetic models involving epistatic interactions, possibly reflecting the complex molecular pathways underlying flowering time (e.g., photoperiod genes; Yang et al. 2013, Blümel et al. 2015, Minow et al. 2018). In this study, genomic variance in Ames-H could not be partitioned reliably by additive, dominance, and epistatic effects, because genomic relationships for pairwise epistatic effects are highly correlated with those for additive effects ($r > 0.99$ between additive and additive×additive relationships). Moreover, epistatic effects in linear mixed models vary depending on how marker variables are centered, in a way that can be arbitrary (Martini et al. 2016, Martini et al. 2017). However, further analyses to investigate the contribution of epistatic effects to genomic variance is merited (Jiang and Reif 2015). Investigating epistatic effects would likely require large panels with more testers, and also efficient methodologies to restrict the number of interactions (e.g., only interactions between homeologs; Santantonio et al. 2019) and the types of effects involved (e.g., only SNP×SNP interactions like additive×additive effects, or SNP×background interactions like SNP×PC effects; Ramstein et al. 2018).

For PH and GY, there is consistent evidence for prevalent dominance effects: (i) significant variance partition by dominance effects (Figure 3a) and (ii) significant linear effects of genomic inbreeding, without any quadratic effect (Figure 3b). Therefore, additive and dominance effects may efficiently capture genetic effects for PH and GY. These results contrast with previous studies on hybrid maize, which showed additive effects could capture most of genotypic variability. Critically, those studies were based on panels derived solely from crosses between different heterotic groups (due to the practical relevance of such crosses), e.g., Flint×Dent (Technow et al. 2014, Giraud et al. 2017) or SS×NSS (Kadam et al. 2016). Therefore, complementation effects were relatively consistent across hybrids and well captured by general

combining abilities, such that variability for specific combining ability was low. In contrast, one of our panels (Ames-H) shows strong variation for complementation effects because it represents a variety of genetic contexts (SS×NSS, SS×SS, Semi-tropical×SS, etc.). Therefore, it is better-suited to represent the differential levels of complementation effects in maize and reveal the importance of dominance effects across maize hybrids.

No QTL effect were detected in Ames-H for PH or GY, whereas previously published analyses have reported significant additive and dominance QTL effects for these traits (Schön et al. 2010, Larièpe et al. 2012). Those studies were based on populations from Design III experiments, where bi-parental progeny (typically RILs) are crossed with either parent. In comparison, panels like Ames-H or even NAM-H are genetically more diverse and are characterized by many low-frequency variants (Figure S3). So, heterogeneity in genetic backgrounds and low variability at markers likely contribute to lower QTL detection power in Ames-H and NAM-H. Moreover, it is possible that the larger QTL effects detected in Design III studies arose from multiple loci in strong linkage, due to relatively few (effective) recombination events in their populations. Consistently, degrees of dominance estimated in those studies were especially large around centromeres, possibly because of repulsion phase linkage (Hill and Robertson 1966). In contrast, genome-wide degrees of dominance estimated in Ames-H are relatively low (< 1) and no significant enrichment for dominance effects is detected in low-recombination regions, after accounting for gene proximity (Table S7). Therefore, differences in QTL detection power between Ames-H and Design III populations may be caused by important differences in both genetic diversity and LD structure.

What is the biological basis for enrichment of SNP effects by gene proximity?

Analyses of functional enrichment point to genetic effects arising mostly from genic regions (proximal SNPs, ≤ 1 kb from annotated genes). The relevance of genic regions for capturing genotypic variability in hybrid maize is consistent with hypotheses about biological causes of heterosis (hybrid vigor) related to gene expression, namely, (i) non-additive inheritance of gene expression and (ii) nonlinear effects of gene expression on agronomic traits (Springer and Stupar 2007, Schnable and Springer 2013). Proposed mechanisms for non-additive inheritance of gene expression include complementation with respect to regulatory motifs or transcription factors, and presence/absence variation (Paschold et al. 2012, Marcon et al. 2017, Zhou et al. 2019), but

studies in maize generally report that most genes have an additive mode of inheritance for expression levels (e.g., Swanson-Wagner et al. 2006, Stupar and Springer 2006, Zhou et al. 2019). Conversely, the gene balance hypothesis indicates that highly connected genes (in pathways, protein complexes, etc.) should be expressed in relative amounts under a stoichiometric optimum (Birchler and Veitia 2010). This optimum points to a balance between benefits of gene expression (from RNA or protein activity) and its costs (from energy requirements and accumulation of wasteful products or toxic intermediates), which may result in nonlinear effects of gene expression (Dekel and Alon 2005, Domingo et al. 2019). Results in support of the gene balance hypothesis in maize include intermediate gene expression harboring minimal burden of deleterious mutations in diverse maize inbred lines (Kremling et al. 2018). Furthermore, models related to metabolic fluxes provide examples of mechanisms by which gene balance can arise (Fiévet et al. 2010, Vacher and Small 2019). These models describe the nonlinear relationships between enzyme concentrations and metabolic fluxes (e.g., hyperbolic functions), so that additive genetic effects on gene expression may translate into non-additive effects on agronomic traits. Importantly, benefits and costs of gene expression are affected by intragenic interactions (e.g., protein folding; Otwinowski et al. 2018), which can be captured by dominance effects and LD within genes, but also intergenic interactions (e.g., pathway interactions, or protein-protein interactions; Vacher and Small 2019, Diss and Lehner 2018), which cannot be captured predictably by dominance effects. Ideally, future research about non-additive genetic effects and their enrichment in genic regions will involve transcriptomic, proteomic and/or metabolomic data, to empirically test the gene balance hypothesis and provide mechanistic explanations for genotypic variability in hybrid maize.

Are dominance effects and enrichments in genic regions useful for genomic prediction?

In this study, the relevance of dominance effects and functional enrichments was evaluated by genomic prediction *across* panels. Therefore, prediction models were assessed for their ability to sustain accuracy across distinct population backgrounds. Genomic prediction accuracy was estimated in NAM-H to reflect genomic selection applications in bi-parental breeding populations crossed to a single tester. These populations serve as useful validation sets because they exemplify inter-heterotic populations, as crosses between PHZ51 (an NSS line) and NAM

inbred lines (related to the SS pool by at least 50% through the common B73 parent). These populations are therefore good examples of breeding populations crossed to a relevant tester. In contrast, genomic prediction accuracy was estimated in Ames-H to reflect a different situation where diverse panels are evaluated for hybrid performance, in genomic prospecting (e.g., for pre-breeding applications; Voss-Fels et al. 2019). Under this validation scheme, validation sets do not correspond to breeding populations, but instead consist of diverse hybrid panels structured by subpopulations and testers (Figure S1).

Enrichment of SNP effects emphasize causal loci; therefore, enrichment procedures such as QTL detection or variance partition can improve the accuracy of genomic prediction models. However, as genetic effects vary between populations, enrichments about small functional classes (e.g., a few GWAS hits) lose their potential. This caveat is exemplified by differences in QTL effects for DTS between Ames-H and NAM-H, and the consequent lack of gain in accuracy by prediction models based on QTL effects (Figure 5; Table S6). Similarly, Spindel et al. (2016) showed benefits of major QTL effects for prediction of flowering time in rice, but only when QTL were detected in the target breeding populations. Contrary to enrichments for QTL, enrichments for larger functional classes (e.g., gene-proximal SNPs) should result in gains of prediction accuracy that are robust to differences in population backgrounds, as is observed here (Figure 5; Table S9). Likewise, Gao et al. (2017) reported gains in genomic prediction accuracy by prioritizing genic SNPs, in mouse, drosophila, and rice (increases in predictive ability averaging +0.013, similar to those realized in this study). Therefore, gains in prediction accuracy by gene proximity should be expected in a broad range of population and species contexts.

While functional enrichments by gene proximity appear beneficial for all traits, incorporating polygenic dominance effects results in gains in prediction accuracy for PH only (Table 2). The lack of gain in prediction accuracy for DTS and GY illustrates possible reasons for disagreement between quality of fit and prediction accuracy often observed in genomic prediction studies. For DTS, incorporating dominance effects results in *statistically* significant improvements in fit, but a genetic model accounting for epistatic interactions appears more plausible according to analyses of QTL and genomic inbreeding. Thus, the choice of prediction procedure should probably come from multiple pieces of evidence in favor of a given genetic model, rather than a single statistical test about the genomic prediction model. In the case of GY,

prediction accuracy across panels is probably hindered by genotype-by-environment interactions, which could be accommodated by models incorporating environmental covariates (e.g., Li et al. 2018, Millet et al. 2019).

Conclusions

Our analyses point to genetic models in hybrid maize which involve interactive effects and emphasize genic regions. While dominance may be relevant to all three traits, other nonlinear effects seemed important for DTS, and interactions with environments appeared critical for GY. Consequently, genomic prediction models were improved by dominance effects for PH only. In contrast, genomic prediction models benefited from functional enrichment in genic regions for all traits. Although gene proximity appeared most useful and meaningful in our study, the value of structural and evolutionary features for genomic prediction deserves more attention. Our results call for further investigation about the biological basis of genetic complementation, and the underlying interactive effects which could enable more robust prediction of genotypic variability in hybrid maize.

ACKNOWLEDGEMENTS

We thank the editor and two anonymous reviewers for their comments which contributed to increase the quality of the manuscript. This work was funded by NSF Plant Genome Program (IOS 0820619 and 1238014) and USDA-ARS. Graduate work of SJL, work of ESE, and IA10 trials were partially funded by Syngenta.

REFERENCES

- Baglama J., and L. Reichel, 2005 Augmented Implicitly Restarted Lanczos Bidiagonalization Methods. *SIAM J. Sci. Comput.* 27: 19–42.
- Bates D., D. Eddelbuettel, and Others, 2013 Fast and elegant numerical linear algebra using the RcppEigen package. *J. Stat. Softw.* 52: 1–24.
- Beissinger T. M., L. Wang, K. Crosby, A. Durvasula, M. B. Hufford, *et al.*, 2016 Recent demography drives changes in linked selection across the maize genome. *Nat Plants* 2: 16084.
- Benjamini Y., and Y. Hochberg, 1995 Controlling the False Discovery Rate: A Practical and Powerful Approach to Multiple Testing. *J. R. Stat. Soc. Series B Stat. Methodol.* 57: 289–300.
- Birchler J. A., and R. A. Veitia, 2010 The gene balance hypothesis: implications for gene

regulation, quantitative traits and evolution. *New Phytol.* 186: 54–62.

Blümel M., N. Dally, and C. Jung, 2015 Flowering time regulation in crops—what did we learn from *Arabidopsis*? *Curr. Opin. Biotechnol.* 32: 121–129.

Bradbury P. J., Z. Zhang, D. E. Kroon, T. M. Casstevens, Y. Ramdoss, *et al.*, 2007 TASSEL: software for association mapping of complex traits in diverse samples. *Bioinformatics* 23: 2633–2635.

Browning B. L., and S. R. Browning, 2009 A unified approach to genotype imputation and haplotype-phase inference for large data sets of trios and unrelated individuals. *Am. J. Hum. Genet.* 84: 210–223.

Browning B. L., Y. Zhou, and S. R. Browning, 2018 A One-Penny Imputed Genome from Next-Generation Reference Panels. *Am. J. Hum. Genet.* 103: 338–348.

Bukowski R., X. Guo, Y. Lu, C. Zou, B. He, *et al.*, 2018 Construction of the third-generation *Zea mays* haplotype map. *Gigascience* 7: 1–12.

Butler D. G., B. R. Cullis, A. R. Gilmour, and B. J. Gogel, 2009 ASReml-R reference manual. The State of Queensland, Department of Primary Industries and Fisheries, Brisbane.

Clifford D., and P. McCullagh, 2005 The regress function. *The Newsletter of the R Project* Volume 6/2, May 2006 39243: 6.

Crow J. F., M. Kimura, and Others, 1970 An introduction to population genetics theory. An introduction to population genetics theory.

Crow J. F., 1998 90 years ago: the beginning of hybrid maize. *Genetics* 148: 923–928.

Davydov E. V., D. L. Goode, M. Sirota, G. M. Cooper, A. Sidow, *et al.*, 2010 Identifying a high fraction of the human genome to be under selective constraint using GERP++. *PLoS Comput. Biol.* 6: e1001025.

Dekel E., and U. Alon, 2005 Optimality and evolutionary tuning of the expression level of a protein. *Nature* 436: 588–592.

Diss G., and B. Lehner, 2018 The genetic landscape of a physical interaction. *Elife* 7. <https://doi.org/10.7554/eLife.32472>

Domingo J., P. Baeza-Centurion, and B. Lehner, 2019 The Causes and Consequences of Genetic Interactions (Epistasis). *Annu. Rev. Genomics Hum. Genet.* 20: 433–460.

Endelman J. B., and J.-L. Jannink, 2012 Shrinkage estimation of the realized relationship matrix. *G3* 2: 1405–1413.

Evans L. M., R. Tahmasbi, S. I. Vrieze, G. R. Abecasis, S. Das, *et al.*, 2018 Comparison of methods that use whole genome data to estimate the heritability and genetic architecture of complex traits. *Nat. Genet.* 50: 737–745.

Falconer D. S., and T. F. C. Mackay, 1996 *Introduction to quantitative genetics*. Harlow, Essex, UK: Longmans Green 3.

Fiévet J. B., C. Dillmann, and D. de Vienne, 2010 Systemic properties of metabolic networks lead to an epistasis-based model for heterosis. *Theor. Appl. Genet.* 120: 463–473.

Flint-Garcia S. A., A.-C. Thuillet, J. Yu, G. Pressoir, S. M. Romero, *et al.*, 2005 Maize association population: a high-resolution platform for quantitative trait locus dissection. *Plant J.* 44: 1054–1064.

Frascaroli E., M. A. Canè, P. Landi, G. Pea, L. Gianfranceschi, *et al.*, 2007 Classical genetic and quantitative trait loci analyses of heterosis in a maize hybrid between two elite inbred lines. *Genetics* 176: 625–644.

Gao N., J. W. R. Martini, Z. Zhang, X. Yuan, H. Zhang, *et al.*, 2017 Incorporating Gene Annotation into Genomic Prediction of Complex Phenotypes. *Genetics* 207: 489–501.

Gardner C. O., 1963 Estimates of genetic parameters in cross-fertilizing plants and their implications in plant breeding. *Statistical genetics and plant breeding* 982: 225–252.

Gerke J. P., J. W. Edwards, K. E. Guill, J. Ross-Ibarra, and M. D. McMullen, 2015 The Genomic Impacts of Drift and Selection for Hybrid Performance in Maize. *Genetics* 201: 1201–1211.

Giraud H., C. Bauland, M. Falque, D. Madur, V. Combes, *et al.*, 2017 Reciprocal Genetics: Identifying QTL for General and Specific Combining Abilities in Hybrids Between Multiparental Populations from Two Maize (*Zea mays* L.) Heterotic Groups. *Genetics* 207: 1167–1180.

Glaubitz J. C., T. M. Casstevens, F. Lu, J. Harriman, R. J. Elshire, *et al.*, 2014 TASSEL-GBS: a high capacity genotyping by sequencing analysis pipeline. *PLoS One* 9: e90346.

Guan Y., and M. Stephens, 2011 Bayesian variable selection regression for genome-wide association studies and other large-scale problems. *Ann. Appl. Stat.* 5: 1780–1815.

Hill W. G., and A. Robertson, 1966 The effect of linkage on limits to artificial selection. *Genet. Res.* 8: 269–294.

Hinze L. L., and K. R. Lamkey, 2003 Absence of epistasis for grain yield in elite maize hybrids. *Crop Sci.* 43: 46–56.

Jarquín D., J. Crossa, X. Lacaze, P. Du Cheyron, J. Daucourt, *et al.*, 2014 A reaction norm model for genomic selection using high-dimensional genomic and environmental data. *Theor. Appl. Genet.* 127: 595–607.

Jiang Y., and J. C. Reif, 2015 Modelling Epistasis in Genomic Selection. *Genetics* 115.177907.

Kadam D. C., S. M. Potts, M. O. Bohn, A. E. Lipka, and A. J. Lorenz, 2016 Genomic Prediction of Single Crosses in the Early Stages of a Maize Hybrid Breeding Pipeline. *G3* 6: 3443–3453.

Kang H. M., J. H. Sul, S. K. Service, N. A. Zaitlen, S.-Y. Kong, *et al.*, 2010 Variance component model to account for sample structure in genome-wide association studies. *Nat. Genet.* 42: 348–354.

Kremling K. A. G., S.-Y. Chen, M.-H. Su, N. K. Lepak, M. C. Romay, *et al.*, 2018 Dysregulation of expression correlates with rare-allele burden and fitness loss in maize. *Nature* 555: 520–523.

Lamkey K. R., and J. W. Edwards, 1999 Quantitative Genetics of Heterosis, pp. 31–48 in *The Genetics and Exploitation of Heterosis in Crops*, American Society of Agronomy, Crop Science Society of America, Madison, WI.

Larièpe A., B. Mangin, S. Jasson, V. Combes, F. Dumas, *et al.*, 2012 The genetic basis of heterosis: multiparental quantitative trait loci mapping reveals contrasted levels of apparent overdominance among traits of agronomical interest in maize (*Zea mays* L.). *Genetics* 190: 795–811.

Larsson S. J., J. A. Peiffer, J. W. Edwards, E. S. Ersoz, S. A. Flint-Garcia, *et al.*, 2017 Genetic Analysis of Lodging in Diverse Maize Hybrids. *bioRxiv* 185769.

Li X., T. Guo, Q. Mu, X. Li, and J. Yu, 2018 Genomic and environmental determinants and their interplay underlying phenotypic plasticity. *Proc. Natl. Acad. Sci. U. S. A.* 115: 6679–6684.

Ma X. Q., J. H. Tang, W. T. Teng, J. B. Yan, Y. J. Meng, *et al.*, 2007 Epistatic interaction is an important genetic basis of grain yield and its components in maize. *Mol. Breed.* 20: 41–51.

Mangin B., A. Siberchicot, S. Nicolas, A. Doligez, P. This, *et al.*, 2012 Novel measures of linkage disequilibrium that correct the bias due to population structure and relatedness. *Heredity* 108: 285–291.

Marcon C., A. Paschold, W. A. Malik, A. Lithio, J. A. Baldauf, *et al.*, 2017 Stability of Single-Parent Gene Expression Complementation in Maize Hybrids upon Water Deficit Stress. *Plant*

Physiol. 173: 1247–1257.

Martinez A. K., J. M. Soriano, R. Tuberosa, R. Koumproglou, T. Jahrmann, *et al.*, 2016 Yield QTLome distribution correlates with gene density in maize. *Plant Sci.* 242: 300–309.

Martini J. W. R., V. Wimmer, M. Erbe, and H. Simianer, 2016 Epistasis and covariance: how gene interaction translates into genomic relationship. *Theor. Appl. Genet.* 129: 963–976.

Martini J. W. R., N. Gao, D. F. Cardoso, V. Wimmer, M. Erbe, *et al.*, 2017 Genomic prediction with epistasis models: on the marker-coding-dependent performance of the extended GBLUP and properties of the categorical epistasis model (CE). *BMC Bioinformatics* 18: 3.

McMullen M. D., S. Kresovich, H. S. Villeda, P. Bradbury, H. Li, *et al.*, 2009 Genetic properties of the maize nested association mapping population. *Science* 325: 737–740.

Mezmouk S., and J. Ross-Ibarra, 2014 The pattern and distribution of deleterious mutations in maize. *G3* 4: 163–171.

Mihaljevic R., H. F. Utz, and A. E. Melchinger, 2005 No Evidence for Epistasis in Hybrid and Per Se Performance of Elite European Flint Maize Inbreds from Generation Means and QTL Analyses. *Crop Sci.* 45: 2605–2613.

Millet E. J., W. Kruijer, A. Coupel-Ledru, S. Alvarez Prado, L. Cabrera-Bosquet, *et al.*, 2019 Genomic prediction of maize yield across European environmental conditions. *Nat. Genet.* 51: 952–956.

Minow M. A. A., L. M. Ávila, K. Turner, E. Ponzoni, I. Mascheretti, *et al.*, 2018 Distinct gene networks modulate floral induction of autonomous maize and photoperiod-dependent teosinte. *J. Exp. Bot.* 69: 2937–2952.

Otwinowski J., D. M. McCandlish, and J. B. Plotkin, 2018 Inferring the shape of global epistasis. *Proc. Natl. Acad. Sci. U. S. A.* 115: E7550–E7558.

Paschold A., Y. Jia, C. Marcon, S. Lund, N. B. Larson, *et al.*, 2012 Complementation contributes to transcriptome complexity in maize (*Zea mays* L.) hybrids relative to their inbred parents. *Genome Res.* 22: 2445–2454.

Ramstein G. P., J. Evans, A. Nandety, M. C. Saha, E. C. Brummer, *et al.*, 2018 Candidate Variants for Additive and Interactive Effects on Bioenergy Traits in Switchgrass (*Panicum virgatum* L.) Identified by Genome-Wide Association Analyses. *Plant Genome* 11.

<https://doi.org/10.3835/plantgenome2018.01.0002>

Reif J. C., A. E. Melchinger, X. C. Xia, M. L. Warburton, D. A. Hoisington, *et al.*, 2003 Genetic

Distance Based on Simple Sequence Repeats and Heterosis in Tropical Maize Populations. *Crop Sci.* 43: 1275–1282.

Reif J. C., A. R. Hallauer, and A. E. Melchinger, 2005 Heterosis and heterotic patterns in maize. *Maydica* 50: 215.

Rodgers-Melnick E., P. J. Bradbury, R. J. Elshire, J. C. Glaubitz, C. B. Acharya, *et al.*, 2015 Recombination in diverse maize is stable, predictable, and associated with genetic load. *Proc. Natl. Acad. Sci. U. S. A.* 112: 3823–3828.

Rodgers-Melnick E., D. L. Vera, H. W. Bass, and E. S. Buckler, 2016 Open chromatin reveals the functional maize genome. *Proc. Natl. Acad. Sci. U. S. A.* 113: E3177–84.

Romay M. C., M. J. Millard, J. C. Glaubitz, J. A. Peiffer, K. L. Swarts, *et al.*, 2013 Comprehensive genotyping of the USA national maize inbred seed bank. *Genome Biol.* 14: R55.

Santantonio N., J.-L. Jannink, and M. Sorrells, 2019 Homeologous Epistasis in Wheat: The Search for an Immortal Hybrid. *Genetics* 211: 1105–1122.

Schadt E. E., S. A. Monks, T. A. Drake, A. J. Lusis, N. Che, *et al.*, 2003 Genetics of gene expression surveyed in maize, mouse and man. *Nature* 422: 297–302.

Schnable P. S., and N. M. Springer, 2013 Progress toward understanding heterosis in crop plants. *Annu. Rev. Plant Biol.* 64: 71–88.

Schön C. C., B. S. Dhillon, H. F. Utz, and A. E. Melchinger, 2010 High congruency of QTL positions for heterosis of grain yield in three crosses of maize. *Theor. Appl. Genet.* 120: 321–332.

Searle S. R., G. Casella, and C. E. McCulloch, 2009 *Variance Components*. John Wiley & Sons.

Shull G. H., 1908 The composition of a field of maize. *J. Hered.* 296–301.

Spindel J. E., H. Begum, D. Akdemir, B. Collard, E. Redoña, *et al.*, 2016 Genome-wide prediction models that incorporate de novo GWAS are a powerful new tool for tropical rice improvement. *Heredity* 116: 395–408.

Springer N. M., and R. M. Stupar, 2007 Allelic variation and heterosis in maize: how do two halves make more than a whole? *Genome Res.* 17: 264–275.

Stupar R. M., and N. M. Springer, 2006 Cis-transcriptional variation in maize inbred lines B73 and Mo17 leads to additive expression patterns in the F1 hybrid. *Genetics* 173: 2199–2210.

Swanson-Wagner R. A., Y. Jia, R. DeCook, L. A. Borsuk, D. Nettleton, *et al.*, 2006 All possible modes of gene action are observed in a global comparison of gene expression in a maize F1

hybrid and its inbred parents. *Proc. Natl. Acad. Sci. U. S. A.* 103: 6805–6810.

Technow F., T. A. Schrag, W. Schipprack, E. Bauer, H. Simianer, *et al.*, 2014 Genome properties and prospects of genomic prediction of hybrid performance in a breeding program of maize. *Genetics* 197: 1343–1355.

Thiemann A., J. Fu, F. Seifert, R. T. Grant-Downton, T. A. Schrag, *et al.*, 2014 Genome-wide meta-analysis of maize heterosis reveals the potential role of additive gene expression at pericentromeric loci. *BMC Plant Biol.* 14: 88.

Vacher M., and I. Small, 2019 Simulation of heterosis in a genome-scale metabolic network provides mechanistic explanations for increased biomass production rates in hybrid plants. *NPJ Syst Biol Appl* 5: 24.

VanRaden P. M., 2008 Efficient methods to compute genomic predictions. *J. Dairy Sci.* 91: 4414–4423.

Voss-Fels K. P., M. Cooper, and B. J. Hayes, 2019 Accelerating crop genetic gains with genomic selection. *Theor. Appl. Genet.* 132: 669–686.

Wallace J. G., P. J. Bradbury, N. Zhang, Y. Gibon, M. Stitt, *et al.*, 2014 Association mapping across numerous traits reveals patterns of functional variation in maize. *PLoS Genet.* 10: e1004845.

Wang L., T. M. Beissinger, A. Lorant, C. Ross-Ibarra, J. Ross-Ibarra, *et al.*, 2017 The interplay of demography and selection during maize domestication and expansion. *Genome Biol.* 18: 215.

Wood S. N., 2003 Thin plate regression splines. *J. R. Stat. Soc. Series B Stat. Methodol.* 65: 95–114.

Yang Q., Z. Li, W. Li, L. Ku, C. Wang, *et al.*, 2013 CACTA-like transposable element in ZmCCT attenuated photoperiod sensitivity and accelerated the postdomestication spread of maize. *Proc. Natl. Acad. Sci. U. S. A.* 110: 16969–16974.

Yang J., S. Mezmouk, A. Baumgarten, E. S. Buckler, K. E. Guill, *et al.*, 2017 Incomplete dominance of deleterious alleles contributes substantially to trait variation and heterosis in maize. *PLoS Genet.* 13: e1007019.

Zhao H., Z. Sun, J. Wang, H. Huang, J.-P. Kocher, *et al.*, 2014 CrossMap: a versatile tool for coordinate conversion between genome assemblies. *Bioinformatics* 30: 1006–1007.

Zhou X., P. Carbonetto, and M. Stephens, 2013 Polygenic modeling with bayesian sparse linear mixed models. *PLoS Genet.* 9: e1003264.

Zhou P., C. N. Hirsch, S. P. Briggs, and N. M. Springer, 2019 Dynamic Patterns of Gene Expression Additivity and Regulatory Variation throughout Maize Development. *Mol. Plant* 12: 410–425.